Hindawi
Journal of Nanomaterials
Volume 2021, Article ID 3913601, 15 pages
https://doi.org/10.1155/2021/3913601

Research Article

Investigations on Microstructure, Mechanical, Thermal, and Tribological Behavior of Cu-MWCNT Composites Processed by Powder Metallurgy

B. Stalin,[1] **M. Ravichandran**,[2] **Alagar Karthick**,[3] **M. Meignanamoorthy**,[2] **G. T. Sudha**,[4] **S. Karunakaran**,[1] **and Murugesan Bharani**[5]

[1]*Department of Mechanical Engineering, Anna University, Regional Campus Madurai, Madurai, 625 019 Tamil Nadu, India*
[2]*Department of Mechanical Engineering, K. Ramakrishnan College of Engineering, Trichy, 621 112 Tamil Nadu, India*
[3]*Department of Electrical and Electronics Engineering, KPR Institute of Engineering and Technology, Coimbatore, 641 407 Tamil Nadu, India*
[4]*Department of Mechanical Engineering, Government Polytechnic College, Coimbatore, 641 014 Tamil Nadu, India*
[5]*School of Textile Leather and Fashion Technology, Kombolcha Institute of Technology, Wollo University, South Wollo, 208 Kombolcha, Ethiopia*

Correspondence should be addressed to Murugesan Bharani; bharani.murugesan@kiot.edu.et

Received 17 June 2021; Revised 5 August 2021; Accepted 13 August 2021; Published 26 August 2021

Academic Editor: Sami-Ullah Rather

Copper (Cu) metal matrix composite (MMC) was developed with multiwall carbon nanotubes (MWCNT) as reinforcement by using powder metallurgy (PM) technique. The composition of the composites is Cu, Cu-4 wt% MWCNT, Cu-8 wt% MWCNT, and Cu-12 wt% MWCNT. The Cu and MWCNTs were blended for 6 hours in a ball mill and compacted at a 6 ton pressure to form green compacts using a 10 ton hydraulic press. Using a tubular furnace, the heat was applied at 900°C for 1.5 hours to impart strength and integrity to the green compacts. Milled composite blends were studied to analyze its characterization through SEM and EDAX analysis. Characterization studies such as SEM and EDAX confirm the presence and even dispersion of Cu and MWCNT constituents. The relative density, hardness, and ultimate compressive strength have been studied, and a remarkable improvement in properties has been obtained by the inclusion of MWCNTs. The composites reinforced by 8 and 12 wt% MWCNT were recorded with low thermal conductivity than the Cu composite reinforced by 4 wt% MWCNT. A wear study was analyzed using Taguchi technique for determining the effect caused by the wear test parameters and MWCNT content on wear rate. The optimized parameter that contributes minimum wear rate was identified as 12 wt% MWCNT content, 10 N applied load, 2 m/s sliding velocity, and 500 m sliding distance. Based on the obtained results, it could be understood that the produced composites can be utilized for various applications like relay contact springs and switchgear, rotor bars, and bus bars.

1. Introduction

Composite fabrication generally incorporates combining the reinforcement with matrix and wetting them. By doing like that, matrix-reinforcement combines collectively into an inflexible material [1]. Because of their superior mechanical, tribological, electrical, and thermal properties, metal matrix composites (MMC) found their widespread applications in ever-growing fields such as aerospace, automotive, and structural [2, 3]. Metal matrix composites (MMCs) are composed of a metallic matrix like Al, Mg, Fe, Cu, and a dispersed ceramic (oxides, carbides, and nitrides). Most MMCs are at a standstill in the improvement stage and are not so extensively established. The merits of MMCs are better strength-to-density ratios, good opposition to wear and corrosion, radiations and fatigue, less creep rate and coefficients of thermal expansion, no moisture absorption, noninflammability, and higher electrical and thermal conductivities [4]. Copper

Table 1: Sample compositions of composite preparation.

Sample no.	Copper (Cu), wt%	Multi-walled carbon nanotube (MWCNT), wt%
1	100	0
2	96	4
3	92	8
4	88	12

has outstanding properties such as electrical conductivity, thermal conductivity, workability, and corrosion resistance. Due to these unique properties, copper is expected to be an outstanding material for manufacturing parts in industries in connection with water supply and electrical and thermal industries and has broad applications in gas turbine nozzles, rocket engines, electrical switches, combustion chamber wall liners, electronic packages, contact breakers, cooling systems, heat exchangers, rotating neutron targets, and integrated circuits. Although copper possesses good properties because of its ductile nature, it has poor mechanical properties and this restricts structural applications [5–7]. To overcome the aforementioned disadvantage, copper is reinforced with Al_2O_3, SiC, TiO_2, Gr, ZrO_2, Ti, TiB, TiB_2, TiC, and fly ash particles to form copper matrix composites which improved the mechanical properties [2, 8–13]. Most manufacturing companies focus on copper matrix composites to produce several components due to the supreme properties over other matrix composites [14]. Carbon nanotubes (CNTs) are such a reinforcement that is well known for its one-dimensional quasicarbon structures with greater aspect ratio and better electrical, thermal, and mechanical properties. The strength of the matrix materials has been found to get improved in association with CNT reinforcements, and hence, the CNT reinforced composites are extensively used in automotive and aerospace applications [15, 16]. In view of the excellent atomic structure and intriguing properties, the researchers heeded over the investigations on CNT. As yet, CNT is the utmost exclusive and adaptable materials exposed in the world, and this has been concluded from the theoretical and experimental results obtained [17]. A substantial attempt to synthesize better Cu-CNT composites is therefore on the rise [18, 19]. Though the powder metallurgy (PM) manufacturing process is an older technique to fabricate MMCs, in the recent era, the manufacturing industries are much attracted towards the PM fabricating process due to the various merits such as components with net shape and no wastages and better mechanical properties [20]. Excellent mechanical properties and fine microstructure can also be achieved without any defects through PM manufacturing process [21, 22].

Liu et al. [23] formed Cu-CNT properties with enhanced strength and ductility, and the better interfacial bonding between Copper and CNT was identified to be the reason behind improved properties. Wang et al. [24] investigated the properties and enhancements of Cu-CNT composites' interfacial interaction and found that yield strength, plasticity, and electrical conductivity were improved with the increase in CNT reinforcement. The predominant increase in yield strength and plasticity was justified by the dislocation theory and the strengthening mechanisms. Yang et al. [25] investigated the mechanical and electrical properties of CNT reinforced copper composites, and the maximum values were obtained in composite with 2.5 vol% CNT reinforcement. Alam et al. [26] studied the wear behavior of stir cast aluminium/SiC nanocomposites and reported that addition of reinforcement increases the wear resistance. Previous reports proven that MWCNTs are remarkably stronger than the impressively single-walled carbon nanotube. Also, the single wall CNT is very useful for electrical and electronics applications. Hence, for strength enhancement, we have used MWCNT as reinforcement in this study.

An extensive literature review indicates that the production of Cu-CNT composites through PM technique is rare. Thus, this study was endeavored to explore the characteristics and properties of Cu-MWCNT composites after developing using the PM method. The influence of MWCNT reinforcement on the hardness, density, compressive strength, and thermal conductivity of the fabricated composites was stated. Wear property of the composites was tested in a pin-on-disc wear tester. The impact of MWCNT weight percentage and the wear test parameters such as load applied, sliding distance, and sliding velocity on the wear rate of Cu-MWCNT composites was analyzed using Taguchi analysis, and the optimized parameter levels for minimum wear rate were also identified.

2. Experimental Details

The chosen copper matrix and MWCNT reinforcement powders of current investigation were procured from Modern Scientific, Madurai, India. The MWCNTs were added to the step of 4, 8, and 12 weight percentages to yield the different compositions. The size of the copper powder is 300 μm, and MWCNT is 50 μm. The proportions of MWCNT particles added to Cu powders to form composites are depicted in Table 1, and the fabrication process setup and sequence of processes used are shown in Figure 1.

In the present investigation, the Cu/MWCNT composites were synthesized through the PM technique as mentioned by the following procedure. At 600 rpm, the mixing of Cu and MWCNTs was achieved by a planetary ball mill with a stainless steel mixing jar consisting of 10 mm diameter stainless steel balls, and the milling was performed for a duration of 6 hours under argon atmosphere. The BPR maintained was 5 : 1, and pure alcohol was added to the mixture so as to control self-cold welding of powders. Milling was also performed to establish reduction in the particle size of powders and thereby improving the homogenization of powders. The density of the used Cu and MWCNT powders was 8.9 g/cc and 1.8 g/cc, respectively, and these density values were considered in the calculation of relative density. Once the milling was complete, each composition was compacted in a hydraulic press with a capacity of 10 Ton. By using a cylindrical punch die arrangement, the well-blended Cu and MWCNT powders were compacted to green compacts of cylindrical shape at room temperature. The compaction was made at a pressure of 6 tons, and the

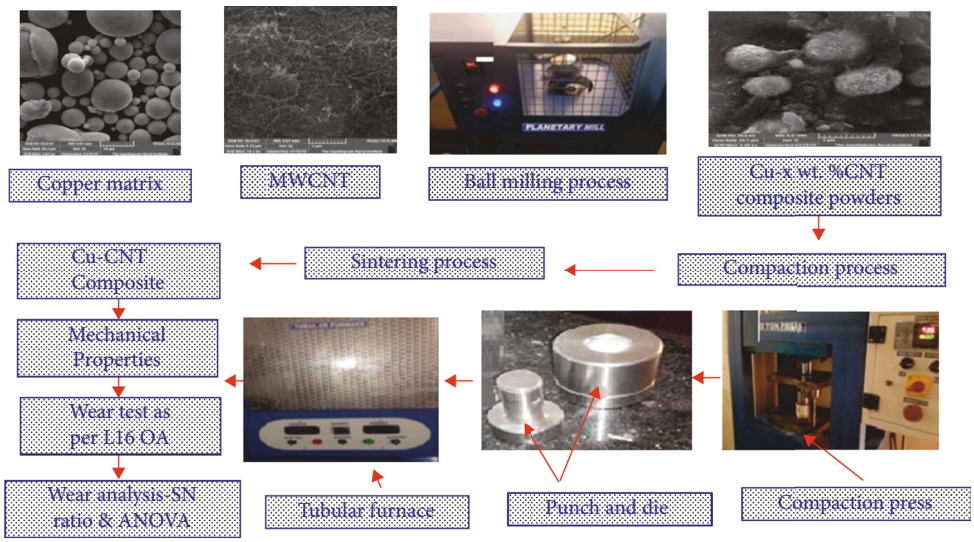

Figure 1: Fabrication process setup and sequence of processes used for the present work.

Table 2: Parameters with levels chosen for wear rate analysis.

Parameters	Symbols	Unit	Level 1	Level 2	Level 3	Level 4
Weight percentage of MWCNT	A	%	0	4	8	12
Load applied	B	N	10	20	30	40
Sliding velocity	C	m/s	1	2	3	4
Sliding distance	D	m	500	1000	1500	2000

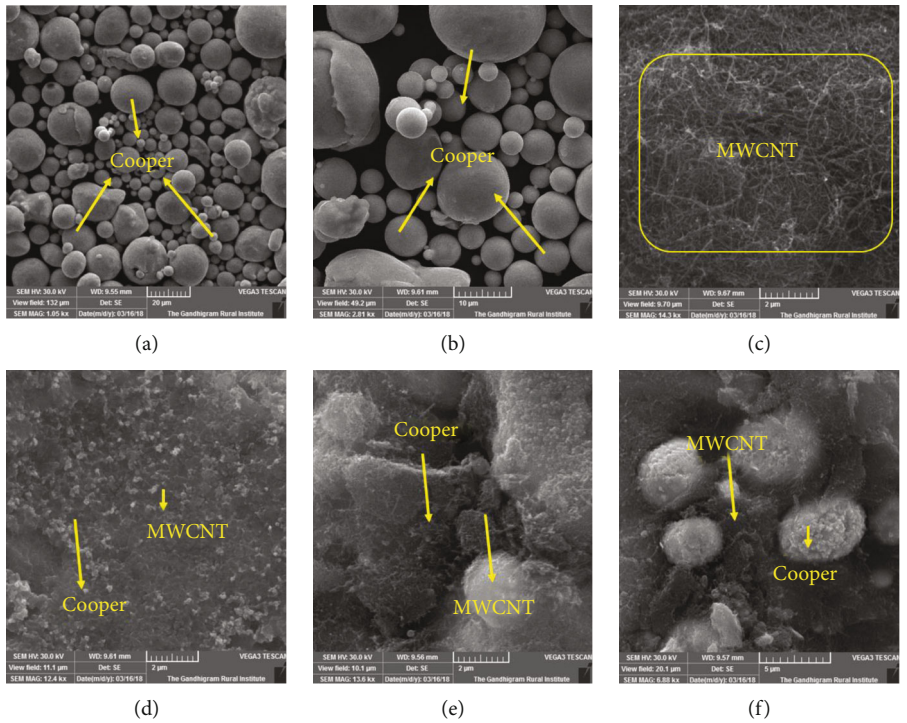

Figure 2: SEM micrographs. (a, b) SEM image of pure copper; (c) SEM image of multiwalled carbon nanotubes; (d) Cu–4 wt% MWCNT; (e) Cu–8 wt% MWCNT; (f) Cu–12 wt% MWCNT milled powders.

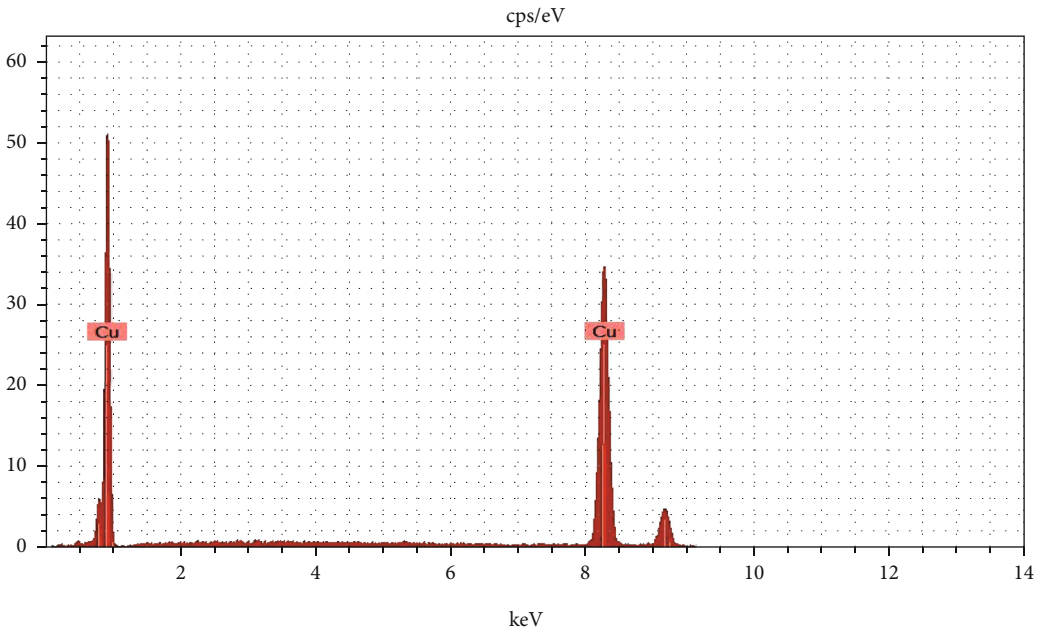

(a)

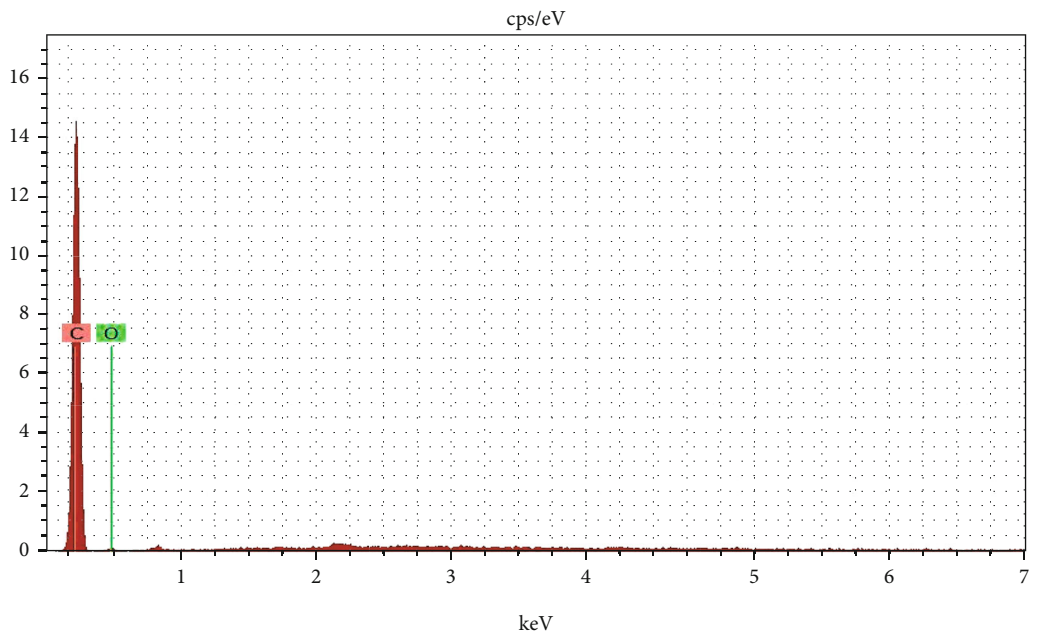

(b)

Figure 3: Continued.

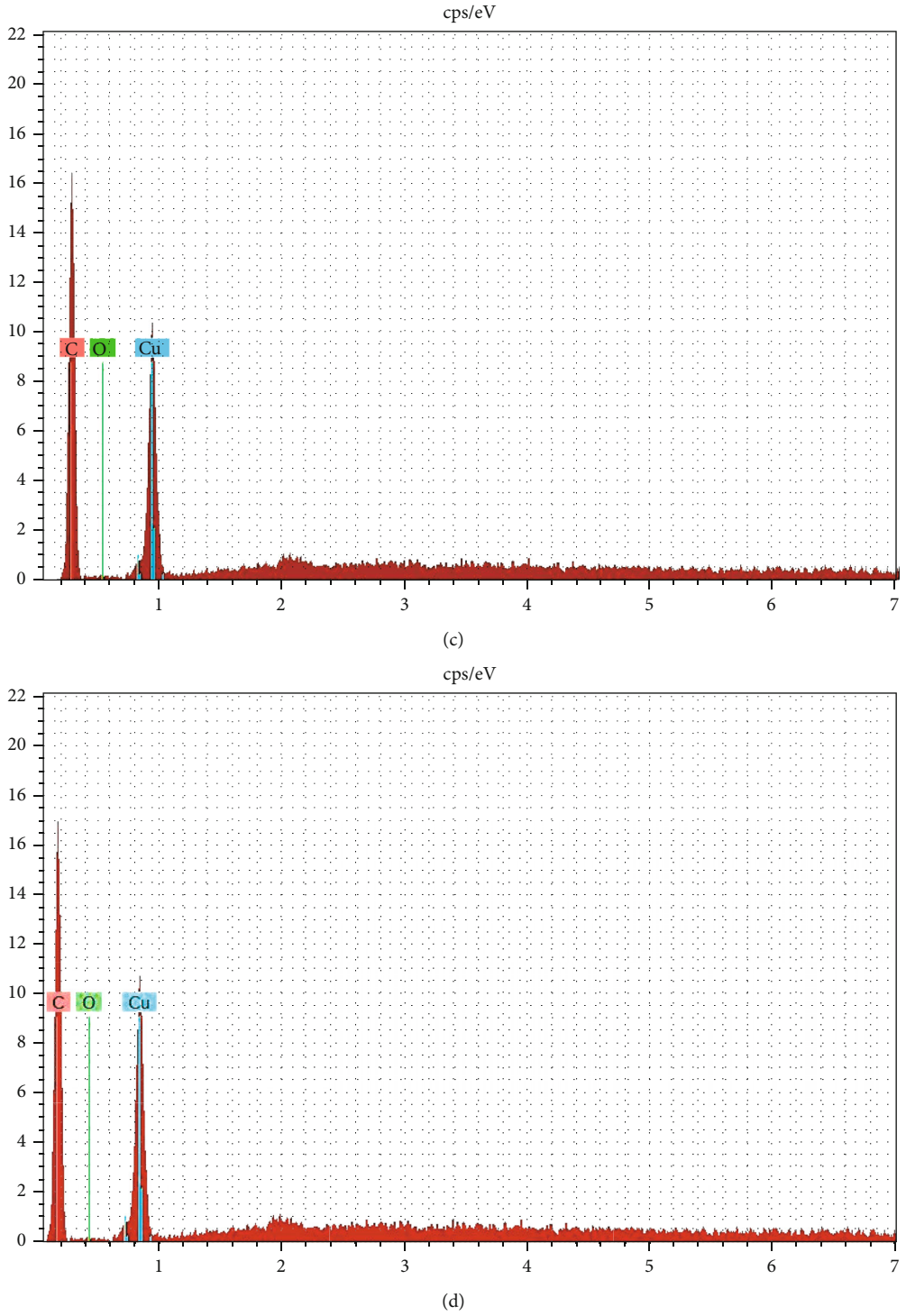

Figure 3: EDX Analysis (a) EDAX of Cu; (b) MWCNT; (c) Cu–4 wt% MWCNT; (d) Cu–8 wt% MWCNT milled powders.

compaction dwell time was about 12 seconds and the resultant cylindrical green compacts were of 10 mm diameter and 10 mm height.

Sintering was done in a tubular furnace at 900°C much below the melting point of copper, to integrate the particles and improve the strength of the green compacts produced. The sintering temperature (900°C) was achieved inside the furnace by heating at a rate of 5°C/min for 1.5 hours. Sintering was performed in a controlled argon atmosphere to produce clean parts without products of oxidation and to prevent surface contamination from atmospheric air. The sintered samples were tested for hardness by using Vickers hardness testing machine by following ASTM standard E384-08 [27]. The compressive strength was evaluated as

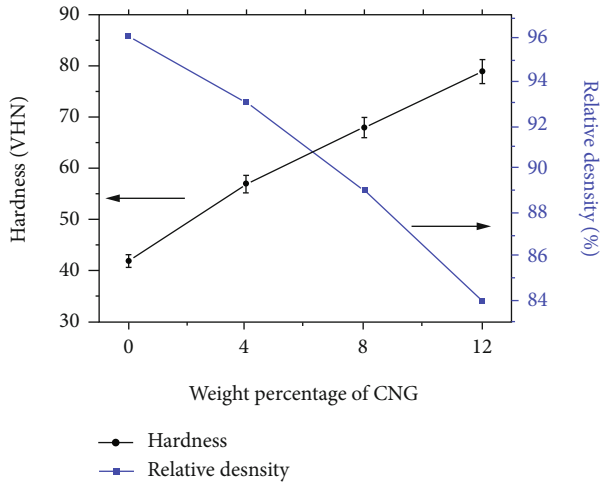

Figure 4: Cu-MWCNT composite hardness and relative density.

per ASTM standard E9-89a using a 10 Ton Universal testing machine [28]. By recording the power meter reading and temperature with respect to time, the thermal conductivity values of the produced composites were determined in W/mK. Three sets of readings were noted for all the experiments, and the average of these three values was calculated for investigation. The wear rate of the composites was evaluated by adopting ASTM G-99 standard procedure using a pin-on-disc apparatus. During experimentation, the Cu-CNT wear test specimens and EN-31 hardened steel with 60 HRC were employed to be the pin and disc material. The surfaces were mirror-polished to enable properly engaged contact between the counterparts and thereby ensuring uniform wear all over the surface. The parameters considered for wear rate analysis were MWCNT weight percentage, load applied, sliding speed, and sliding distance, and for each parameter, four levels were chosen as depicted in Table 2. By L16 orthogonal array, the experimental run for the study was framed and the effect of these parameters on the wear rate was analyzed by Taguchi analysis.

3. Results and Discussion

3.1. Microstructural Characterization. As obtained, pure Cu powder was subjected to SEM examination and the micrographs that clearly illustrate the three-dimensional spherical shaped copper powder particles are shown in Figures 2(a) and 2(b). Figure 2(c) reveals the needle-like one-dimensional acicular-shaped MWCNT powder particles. Figures 2(d)–2(f) exhibit the SEM micrograph of the Cu + 4 wt%MWCNT, Cu + 8 wt%MWCNT, and Cu + 12 wt %CNT milled powders. The occurrence of CNT particle is evidently noticeable in all the samples of Figures 2(d)–2(f). The SEM image in Figure 2(d) shows that the MWCNT particulates were more evenly distributed among the copper particles and are homogenous. Figures 2(e) and 2(f) reveal the occurrence of MWCNT clusters in between the copper matrixes in Cu–8 wt% MWCNT and Cu–12 wt% MWCNT composites, and this confirms the possibility of reinforcement accumulation formation at higher reinforcement content. The shape change effect and cold welding [29] of MWCNT with copper particles that happened during ball milling were understood from Figures 2(e) and 2(f).

3.2. Energy Dispersive X-Ray Analysis. The compositional analysis of the As procured pure Cu and MWCNT powders, and milled Cu-MWCNT powders were done by EDAX, and the result supplements the even dispersal observation made by SEM micrographs. The images displayed in Figures 3(a)–3(d) indicate the occurrence of peaks equivalent to the presence of pure Cu and MWCNT. The higher peaks correspond to the main content copper in the composite powders. The even mixing and homogenous dispersal of MWCNT particles in Cu particles were substantiated by the obtained MWCNT weight percentage from Figures 3(c) and 3(d).

3.3. Relative Density and Hardness of Cu-MWCNT Composites. The theoretical and experimental density of the composites was calculated by following the rule of mixtures and Archimedes principle, respectively. From the calculated values, the relative density values of the copper and Cu-MWCNT composites were calculated. The relative density of the composites was depicted in the graph notified in Figure 4. From the graph in Figure 4, it was noted that the relative density values declined with the addition of more MWCNT content and the Cu-12% MWCNT composite exhibited the lowest relative density values. Increasing the wt% of MWCNT beyond 10 causes severe decline in the curve, and this severe declining effect on the relative density may be possible because of the accumulation of CNT particles at a higher reinforcement weight percentage that causes deprived bonding of CNT with the Cu matrix [16].

Figure 4 also depicts the hardness of copper and Cu-MWCNT composites with respect to the different MWCNT percentages loaded, and the hardness values were found to get enhanced with the increase in MWCNT content. The hardness enhancement is accredited to the strengthening effect imposed by the dispersal of highly strengthened MWCNT particles in the copper matrix. The increased amount of CNT particles with high strength enhanced the hardness of the composite progressively [30]. The increase in hardness improved the bonding between the copper and MWCNT particles. Numerous researchers investigated and explained the correlation that exists between the hardness and strengthening effect of the CNT-embodied composites. Akbarpour et al. [27] fabricated CNT-reinforced composites with elevated hardness values, and the hardness improvement with incorporation of CNT particles may be due to the underlying conditions: (i) reduction in grain size, (ii) increase in dislocation density, (iii) decrease in pore size, and (iv) work hardening of powders during milling. Besides outstanding interfacial bonding, hardness may be improved because of the prevention of dislocation movement due to CNT inclusion as per Hall-patch and Orowan strengthening phenomena. The improvement of hardness in Cu-CNT composites is due to excellent physical bonding between Cu and CNT at the interface. Due to grain improvement, particle strengthening and load bearing ability of hard

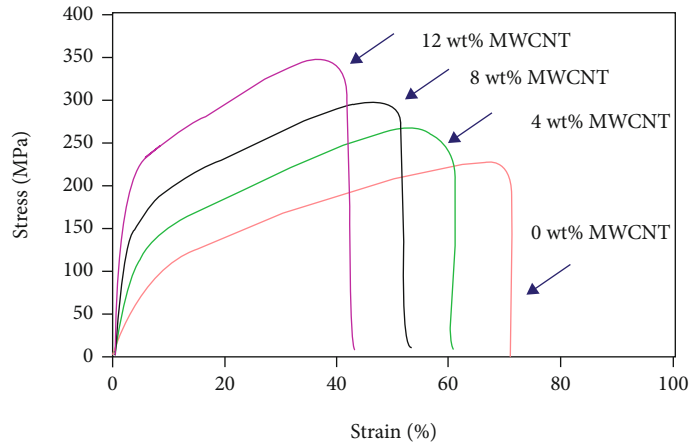

Figure 5: Stress-strain curve of Cu-MWCNT composite.

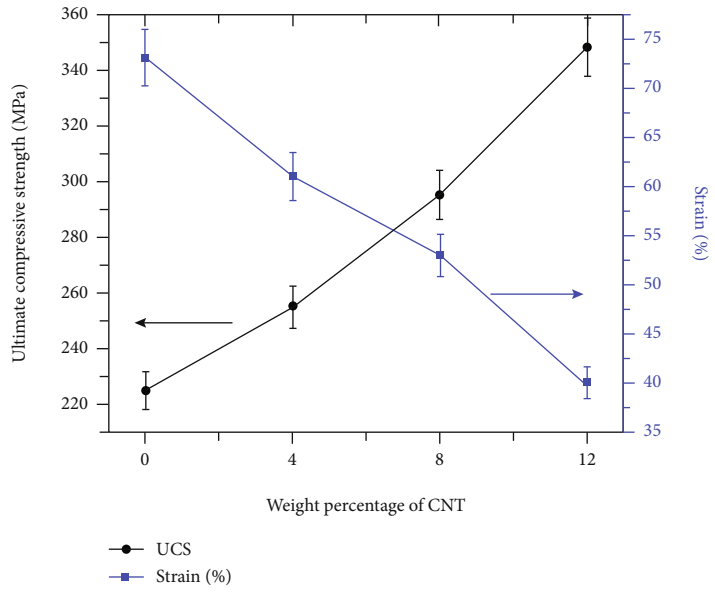

Figure 6: Effect of Cu-MWCNT on compression strength.

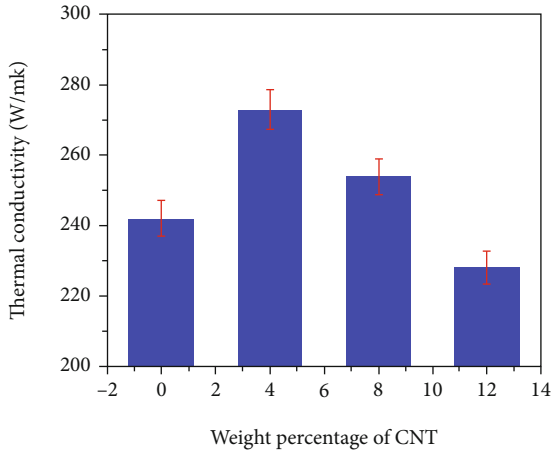

Figure 7: Effect of Cu-MWCNT on thermal conductivity.

reinforcement particle with matrix composites hardness enhanced [31].

3.4. Compressive Strength. The stress-strain curves drawn out with the values attained from the compression test carried out on Cu, Cu–4 wt% MWCNT, Cu–8 wt% MWCNT, and Cu–12 wt% MWCNT composites are illustrated in Figure 5. The compression strength of the Cu-MWCNT composites was better when compared with copper and on account of the progressive inclusion of MWCNT reinforcement; 33% enhancement in compressive strength was recorded. The superior molecular level mixing of matrix and reinforcement particles and the occurrence of better distribution impacted the stress-strain relationship [30]. The occurrence of strengthening accompanied by the load transfer between the copper and high strength MWCNT particles at their interfaces also leads to improvement in compressive strength of the composites. The fact that

Table 3: Wear rate and their corresponding *S*/*N* ratio.

Experiment number	Weight percentage of MWCNT	Applied load (N)	Sliding velocity (m/s)	Sliding distance (m)	Wear rate $(mm^3/Nm) \times 10^{-6}$	*S*/*N* ratio
1	0	10	1	500	44.59	-32.9847
2	0	20	2	1000	48.62	-33.7363
3	0	30	3	1500	53.49	-34.5655
4	0	40	4	2000	57.64	-35.2145
5	4	10	2	1500	26.95	-28.6112
6	4	20	1	2000	29.54	-29.4082
7	4	30	4	500	33.52	-30.5061
8	4	40	3	1000	36.74	-31.3028
9	8	10	3	2000	7.13	-17.0618
10	8	20	4	1500	10.77	-20.6443
11	8	30	1	1000	17.55	-24.8855
12	8	40	2	500	13.92	-22.8728
13	12	10	4	1000	4.59	-13.2363
14	12	20	3	500	4.12	-12.2979
15	12	30	2	2000	5.16	-14.253
16	12	40	1	1500	6.47	-16.2181

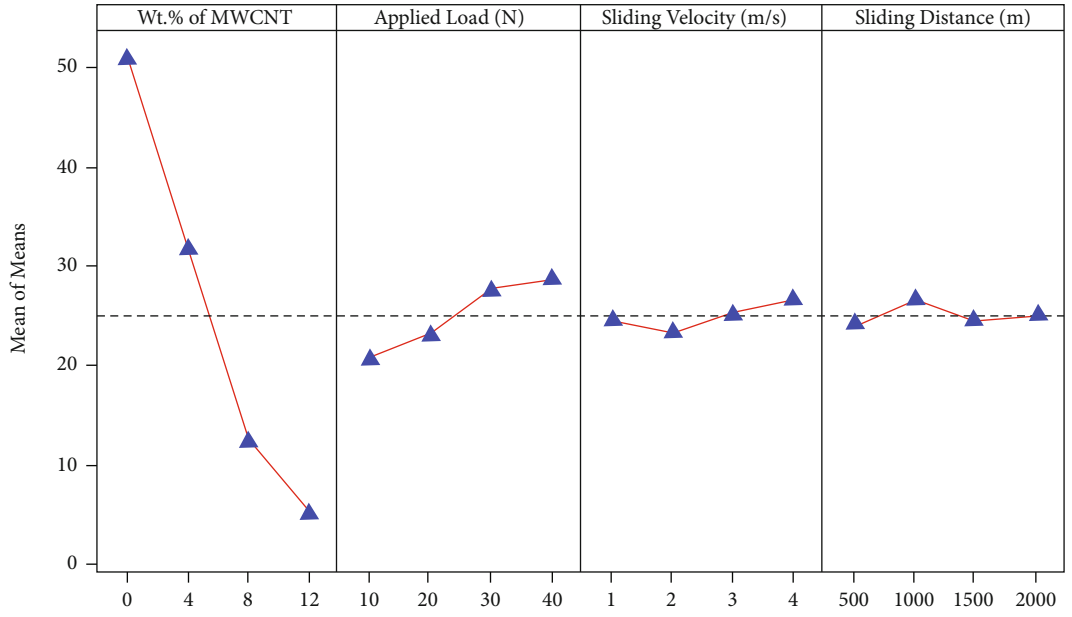

Figure 8: Main effect plot for mean (wear rate).

enhanced dislocation density tends to improve the compressive properties was because of thermal mismatch between matrix and reinforcement [32] and Orowan strengthening mechanism and dispersion hardening effect [33].

Figure 6 shows that the ultimate compressive strength increases with increasing MWCNT reinforcement weight percentage, and the results implied that the compressive strength of Cu-MWCNT composites was superior than the copper matrix. The augmentation of ultimate compressive strength was because of the noteworthy causes such as grain refinement, load transfer from Cu matrix to MWCNT reinforcement, and Orowan strengthening mechanism. Higher plastic deformation and strain hardening also contributed to greater compression strength. It is also well proved by many researchers that the addition of reinforcement content improves the compressive strength [15, 17]. The main significant cause for compressive strength improvement is well and fine dispersion of MWCNT particles with matrix.

3.5. Thermal Conductivity. Figure 7 depicts the influence made by the MWCNT reinforcement particles on the thermal conductivity Cu-MWCNT composites. The graph illustrated that the maximum thermal conductivity was recorded with the composite having 4 wt% MWCNT. The uniform

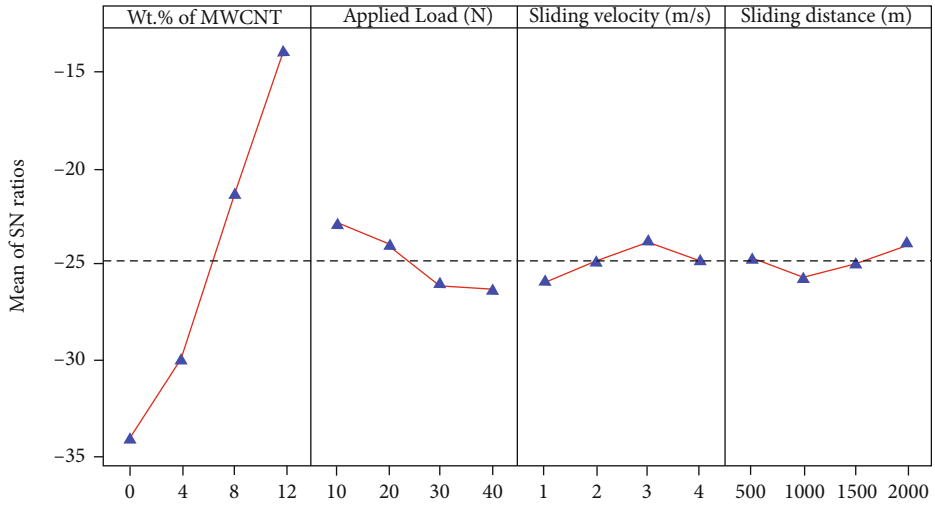

Figure 9: Main effect plot for *S/N* ratios (wear rate).

Table 4: Response table for the signal to noise ratios (smaller is better).

Level	Weight percentage of MWCNT	Applied load (N)	Sliding velocity (m/s)	Sliding distance (m)
1	-34.13	-22.97	-25.87	-24.67
2	-29.96	-24.02	-24.87	-25.79
3	-21.37	-26.05	-23.81	-25.01
4	-14.00	-26.40	-24.90	-23.98
Delta	20.12	3.43	2.07	1.81
Rank	1	2	3	4

Table 5: Response table for means.

Level	Weight percentage of MWCNT	Applied load (N)	Sliding velocity (m/s)	Sliding distance (m)
1	51.085	20.815	24.537	24.038
2	31.688	23.262	23.662	26.875
3	12.343	27.430	25.370	24.420
4	5.085	28.692	26.630	24.868
Delta	46.000	7.877	2.968	2.837
Rank	1	2	3	4

and even dispersion of MWCNT reinforcement and also the existence of better interfacial bonding contributed to the improvement in thermal conductivity. Beyond 4 wt%, the addition of MWCNT particles and the thermal conductivity experiences the reverse trend and declines with the addition of 8 and 12 wt% MWCNT reinforcement particles. Furthermore, increasing the MWCNT weight percentage up to 12 wt%, the thermal conductivity value decreases drastically. This significant lessening of thermal conducting property with the more weight percentage of MWCNT reinforcement addition is justified by the following reasons:

(i) The agglomerated MWCNTs which were held together as a bunch failed to maintain the contact with the copper matrix, and hence, the higher weight percentage of MWCNTs cannot subsidize the thermal conducting effect

(ii) An agglomeration of MWCNT may tempt the tube-tube interface, and this bundling separates the CNTs into ropes and offers the inner tube dispersion of phonons; therefore, a noteworthy reduction in the thermal conductivity occurred [28, 34]

(iii) The heat flow transformation in the composites was hindered due to the back dispersion of phonons in the composites which were caused by clustering effect [35]. Nevertheless, in this study, it is clear that thermal conductivity of copper matrix is superior than MWCNT particle; this is the most important reason to beg off in the composite thermal conductivity

3.6. Taguchi Analysis: Wear Rate versus wt% of MWCNT, Applied Load, Sliding Velocity, and Sliding Distance. This wear study conducted to determine the optimized parameter levels for achieving the minimum wear rate followed the L16 orthogonal array, and the experimental values acquired were interpreted using MINITAB software. The optimization is done by spotting the level of the parameter that yields the preferred quality characteristic, and for the current investigation, "the smaller the better" quality characteristic was chosen. The experimental observations are shown in Table 3, and the *S/N* ratios are obtained by dividing the mean (signal) to the standard deviation (noise). The maximum wear rate of 57.64×10^{-6} (mm^3/Nm) was recorded by the pure copper without MWCNT particles, and the minimum wear rate of 4.12×10^{-6} (mm^3/Nm) was observed in the sample with 12 wt% MWCNT. These values illustrate the leading control exhibited by the percentage of MWCNT reinforcement over the wear rate of the Cu-MWCNT composites. The property wear resistance is always related and directly proportional to its hardness as indicated by Archard's law [36]. The high hardness exhibited by the composite

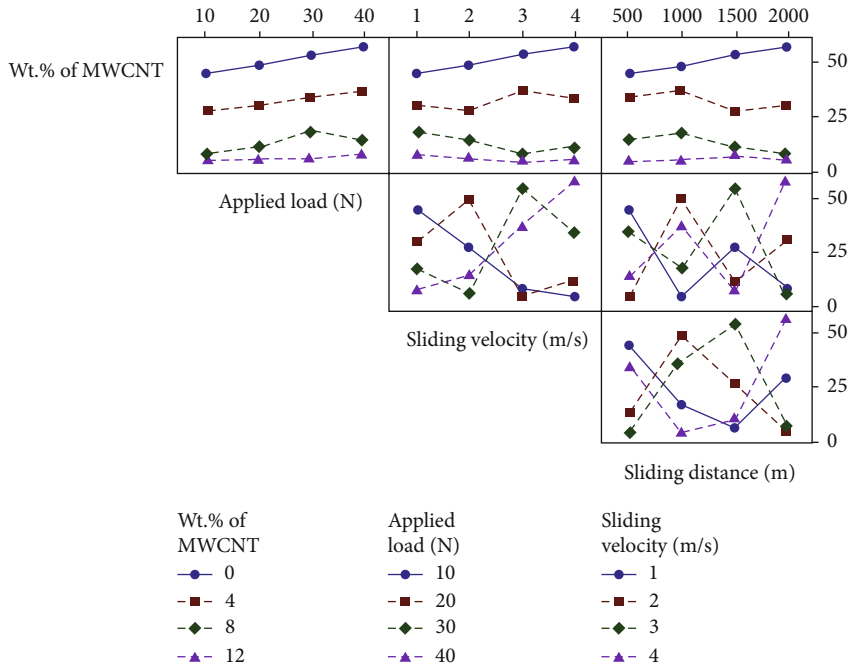

Figure 10: Interaction plot showing the interaction effect caused by input parameters on wear rate.

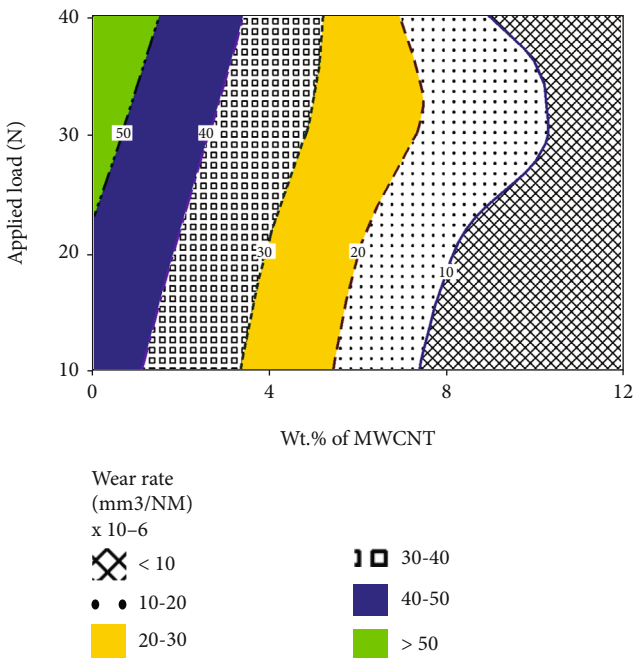

Figure 11: Contour plot showing wear rate with the combined effect of wt% of MWCNT and applied load.

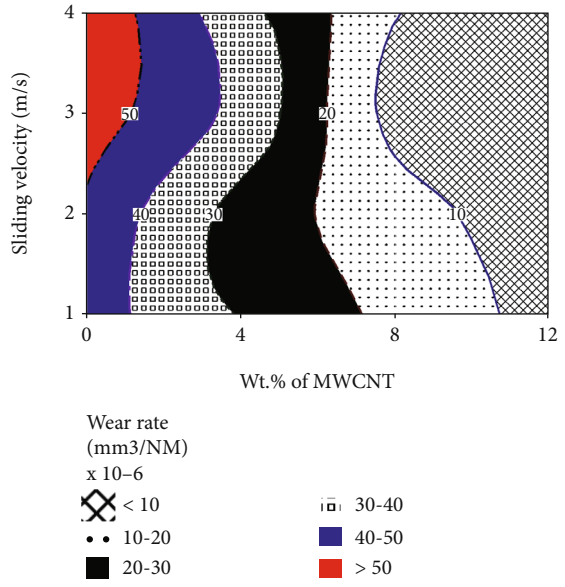

Figure 12: Contour plot showing wear rate with the combined effect of wt% of MWCNT and sliding velocity.

with 12 wt% MWCNT thereby explicates its high wear resistance behavior.

The main effect plots portray the influence made by the process input parameters over the response. The nature of lines observed in the main effect plot elucidates the influence level. The parameter that contributes a highly inclined line will be proclaimed as the most influential parameter, and the parameter with a plot nearer to the horizontal axis will be the least influential one. From the plots in Figures 8 and 9, the addition of MWNT wt% was recognized to be the predominant parameter to affect wear rate. The parameters sliding velocity and sliding distance were recognized as the least significant parameters. These results were also substantiated by the delta and rank values in Tables 4 and 5. The parameter wt% of MWCNT with the highest rank is the most significant parameter followed by applied load, sliding velocity, and sliding distance. From the main effect plots, the optimized parameter levels that contribute minimum wear rate were identified as 12% MWCNT content, 10 N applied load,

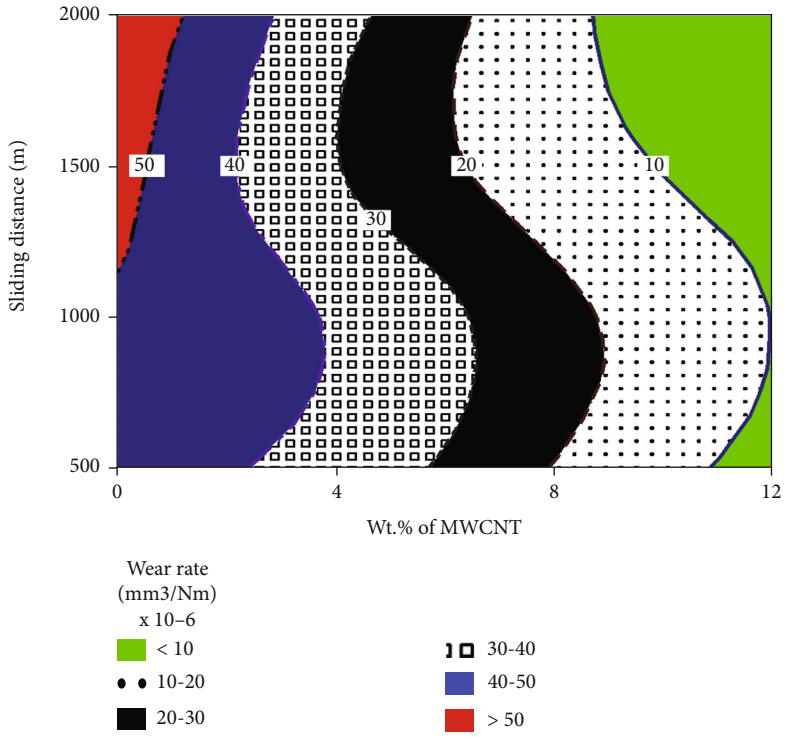

Figure 13: Contour plot showing wear rate with the combined effect of wt% of MWCNT and sliding distance.

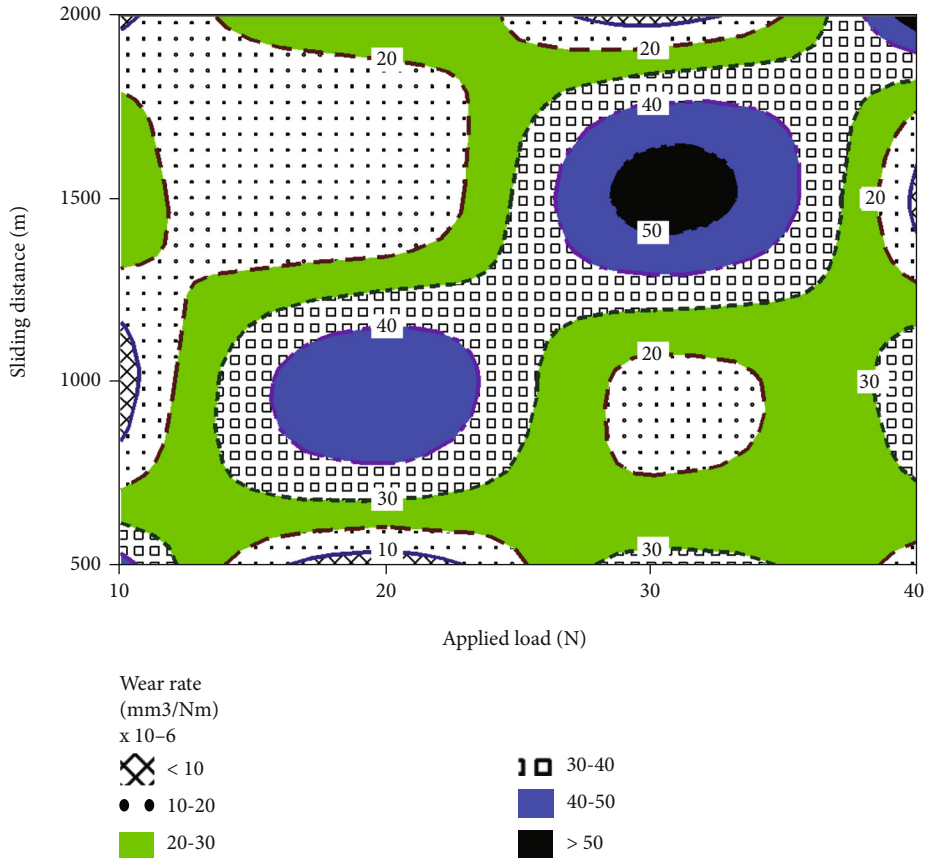

Figure 14: Contour plot showing wear rate with the combined effect of applied load and sliding distance.

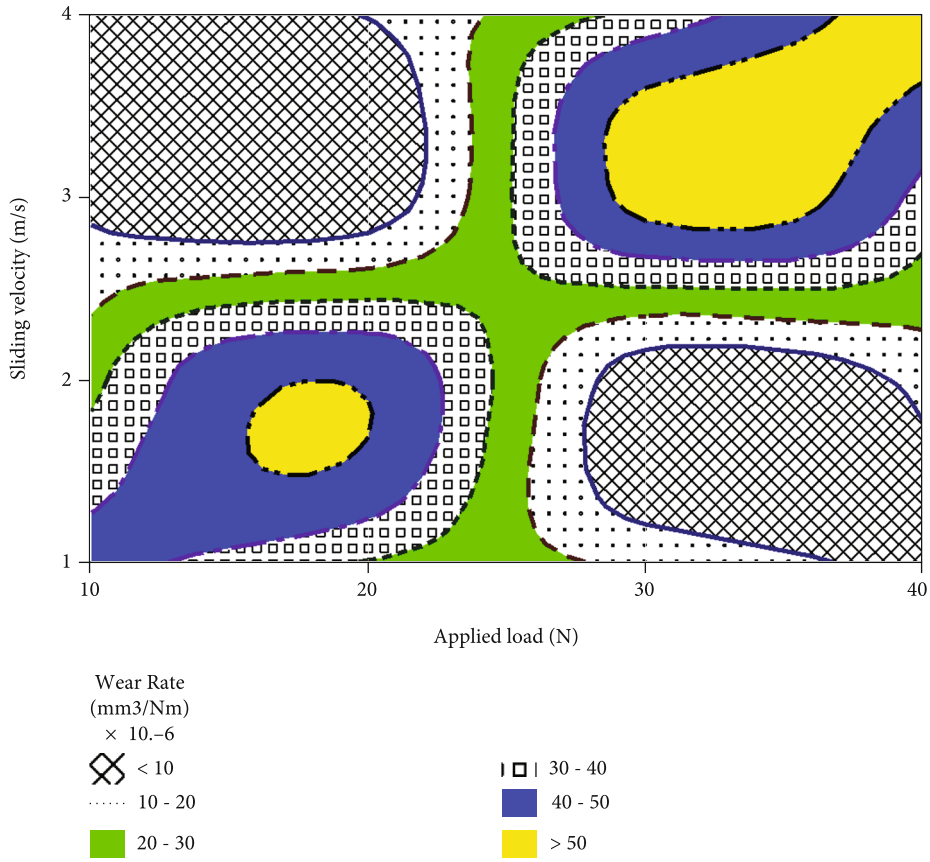

Figure 15: Contour plot showing wear rate with the combined effect of applied load and sliding velocity.

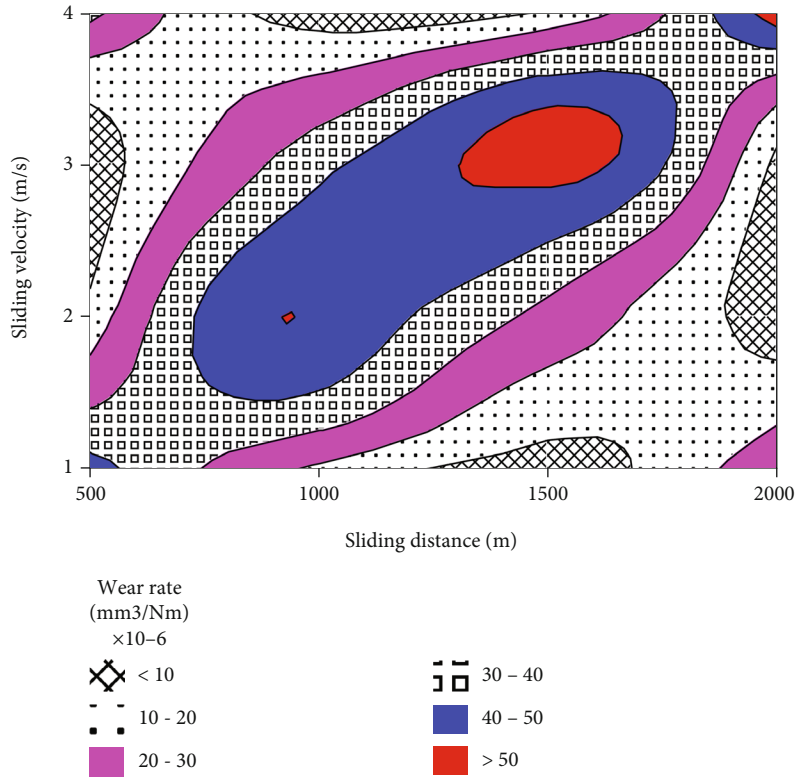

Figure 16: Contour plot showing wear rate with the combined effect of sliding distance and sliding velocity.

Table 6: Analysis of variance for wear rate $(mm^3/Nm) \times 10^{-6}$.

Source	DF	Seq SS	Adj SS	Adj MS	*F*-value	*P* value	% contribution
Weight percentage of MWCNT	3	5127.84	5127.84	1709.28	305.89	≤0.001	95.97
Applied load (N)	3	160.25	160.25	53.42	9.56	0.048	2.99
Sliding velocity (m/s)	3	19.15	19.15	6.38	1.14	0.458	0.35
Sliding distance (m)	3	19.14	19.14	6.38	1.14	0.458	0.35
Error	3	16.76	16.76	5.59			
Total	15	5343.14					

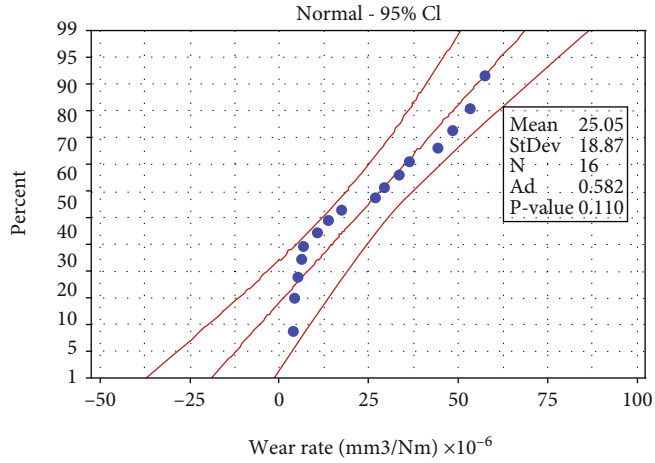

Figure 17: Probability plot.

2 m/s sliding velocity, and 500 m sliding distance. The similar results were observed for the researcher [2]. The rise in sliding and sliding speed rises the temperature amid the counterparts and therefore successfully improves wear rate. An augmentation in the value of applied load contact amid disc and pin rises causes the wear rate to get prominent [37].

The interaction effect generated from various combinations of input parameters and the effect imposed on the wear rate was as illustrated in the interaction plot in Figure 10. The parallel lines perceived in the frontline plots reveal that no interaction effect was caused by the wt% of MWCNT when linked with the other three parameters. Under all cases, the composite with 12 wt% MWNCT gained the minimum wear rate. The wear rate gets elevated because of the hike in applied load, and this may be attributed to the perfect contact and in turn the friction between the counterparts encountered at high loads. Also, the plastic deformation was configured due to the existence of friction-induced high temperature contributed to the increase in wear loss.

Though the sliding distance was drawn out to be the least significant factor, the spike in sliding distance increases the wear rate initially, then suddenly experiences a drop-in wear rate, and resumes the increasing trend. This behavior can be well explained by correlating with the oxide layer formation. An increase in sliding distance will bring out more heat between the mating parts, and this aids in oxide layer formation that inhibits the wear loss. For a further increase in sliding distance, due to high temperature, the mating surfaces become softer and the oxide layer deteriorates causing the wear rate to get increased again. The cross-linked patterns observed in the interaction plots that portray the combined effect of applied load, sliding distance, and sliding velocity revealed the presence of interaction effect between the aforesaid parameters. The contour plots in Figures 11–13 explain the combined effect caused by the weight percentage of MWCNT when interacted with load, sliding velocity, and sliding distance. In all the three plots, lower wear rate region was observed in the zone with 12 wt% MWCNT and the pure copper contributes to the high wear rate region. The *y*-axis parameters remain ineffective and failed to cause the combined effect. The scattered low wear rate region in Figures 14–16 confirms the presence of interaction effect between the respective parameters.

3.7. ANOVA Analysis of Wear Rate. Through ANOVA (Table 6), by conducting *F*-test and identifying the maximum *F*-value, the most influencing parameter can be ascertained. The weight percentage scored a maximum *F*-value of 305.89 and succeeded to be the most influencing parameter. The parameters sliding velocity and sliding distance were proven progressive inclusion of MWCNT reinforcement to be the least significant with 1.14 as the *F*-value.

The probability plot in Figure 17 confirmed that the process pursued a normal distribution and also verified the absence of outliers. These observations inferred that the model proposed for wear study was executed satisfactorily.

4. Conclusions

Cu-MWCNT composites were successfully produced via powder metallurgy route, and the impact made by MWCNT on the behaviours of the composite was studied. The physical and mechanical properties of the Cu-MWCNT composites were evaluated and by performing Taguchi analysis, the effect of wear test parameters and the optimized conditions to accomplish minimum wear rate were identified. From the results of the current investigation, the following conclusions were made:

(i) The SEM micrographs of the milled composite powders confirm even dispersal of the composite constituents and proved 6 hours of milling to be an effective and optimum milling time to achieve the aforesaid condition

(ii) The existence of Cu and MWCNT particles in the composite powders formed was confirmed by EDAX analysis

(iii) Relative density values show the occurrence of agglomerated MWCNT with higher reinforcement addition

(iv) The hardness and compressive strength of the composites were superior over pure copper matrix, and the highest values were attained in the composites with the addition of 12 wt% of MWCNT

(v) The MWCNT addition was limited to 4 wt%, and while increasing further up to 12 wt%, the thermal conductivity of the composites was found to get declined due to cluster formation

(vi) The pure copper exhibits the maximum wear rate, and the MWCNT reinforcement weight content was identified as the most significant parameter

(vii) The optimized parameter levels that contribute minimum wear rate were identified as 12% MWCNT content, 10 N applied load, 2 m/s sliding velocity, and 500 m sliding distance

Data Availability

The data used to support the findings of this study are included in the article.

Conflicts of Interest

The authors declare that there is no conflict of interest regarding the publication of this article.

References

[1] M. T. Alam, A. H. Ansari, S. Arif, and M. N. Alam, "Mechanical properties and morphology of aluminium metal matrix nanocomposites-stir cast products," *Advances in Materials and Processing Technologies*, vol. 3, no. 4, pp. 600–615, 2017.

[2] B. Stalin, M. Ravichandran, G. T. Sudha et al., "Effect of titanium diboride ceramic particles on mechanical and wear behaviour of Cu-10 wt% W alloy composites processed by P/M route," *Vacuum*, vol. 184, article 109895, 2021.

[3] Y. Liu, F. Wang, Y. Cao et al., "Unique defect evolution during the plastic deformation of a metal matrix composite," *Scripta Materialia*, vol. 162, pp. 316–320, 2019.

[4] M. T. Alam, S. Arif, A. H. Ansari, and M. N. Alam, "Optimization of wear behaviour using Taguchi and ANN of fabricated aluminium matrix nanocomposites by two-step stir casting," *Materials Research Express*, vol. 6, no. 6, article 065002, 2019.

[5] X. Gao, H. Yue, E. Guo et al., "Tribological properties of copper matrix composites reinforced with homogeneously dispersed graphene nanosheets," *Journal of Materials Science & Technology*, vol. 34, no. 10, pp. 1925–1931, 2018.

[6] T. Zuo, J. Li, Z. Gao et al., "Simultaneous improvement of electrical conductivity and mechanical property of Cr doped Cu/CNTs composites," *Materials Today Communications*, vol. 23, article 100907, 2020.

[7] K. R. Ramkumar, S. Ilangovan, S. Sivasankaran, and A. S. Alaboodi, "Experimental investigation on synthesis and structural characterization of Cu- Zn-x wt%Al_2O_3 (x = 0, 3, 6, 9 & 12%) nanocomposites powders through mechanical alloying," *Journal of Alloys and Compounds*, vol. 688, pp. 518–526, 2016.

[8] S. D. Kumar, M. Ravichandran, A. Jeevika, B. Stalin, C. Kailasanathan, and A. Karthick, "Effect of ZrB_2 on microstructural, mechanical and corrosion behaviour of aluminium (AA7178) alloy matrix composite prepared by the stir casting route," *Ceramics International*, vol. 47, no. 9, pp. 12951–12962, 2021.

[9] S. Sebastin, A. K. Priya, A. Karthick, R. Sathyamurthy, and A. Ghosh, "Agro waste sugarcane bagasse as a cementitious material for reactive powder concrete," *Clean Technologies*, vol. 2, no. 4, pp. 476–491, 2020.

[10] E. Karakulak, "Characterization of Cu–Ti powder metallurgical materials," *International Journal of Minerals, Metallurgy, and Materials*, vol. 24, no. 1, pp. 83–90, 2017.

[11] K. J. Joshua, S. J. Vijay, and D. P. Selvaraj, "Effect of nano TiO_2 particles on microhardness and microstructural behavior of AA7068 metal matrix composites," *Ceramics International*, vol. 44, no. 17, pp. 20774–20781, 2018.

[12] S. Liang, W. Li, Y. Jiang, F. Cao, G. Dong, and P. Xiao, "Microstructures and properties of hybrid copper matrix composites reinforced by TiB whiskers and TiB_2 particles," *Journal of Alloys and Compounds*, vol. 797, pp. 589–594, 2019.

[13] R. G. Chandrakanth, K. Rajkumar, and S. Aravindan, "Fabrication of copper–TiC–graphite hybrid metal matrix composites through microwave processing," *The International Journal of Advanced Manufacturing Technology*, vol. 48, no. 5-8, pp. 645–653, 2010.

[14] K. R. Ramkumar, S. Sivasankaran, and A. S. Alaboodi, "Effect of alumina content on microstructures, mechanical, wear and machining behavior of Cu-10Zn nanocomposite prepared by mechanical alloying and hot- pressing," *Journal of Alloys and Compounds*, vol. 709, pp. 129–141, 2017.

[15] D. Jeyasimman, K. Sivaprasad, S. Sivasankaran, and R. Narayanasamy, "Fabrication and consolidation behavior of Al 6061 nanocomposite powders reinforced by multi-walled carbon nanotubes," *Powder Technology*, vol. 258, pp. 189–197, 2014.

[16] V. Kavimani, B. Stalin, P. M. Gopal, M. Ravichandran, A. Karthick, and M. Bharani, "Application of r-GO-MMT hybrid nanofillers for improving strength and flame retardancy of epoxy/glass fibre composites," *Advances in Polymer Technology*, vol. 2021, Article ID 6627743, 9 pages, 2021.

[17] S. M. Uddin, T. Mahmud, C. Wolf et al., "Effect of size and shape of metal particles to improve hardness and electrical properties of carbon nanotube reinforced copper and copper alloy composites," *Composites Science and Technology*, vol. 70, no. 16, pp. 2253–2257, 2010.

[18] S. K. Soni, B. Thomas, and V. R. Kar, "A comprehensive review on CNTs and CNT-reinforced composites: syntheses, characteristics and applications," *Materials Today Communications*, vol. 25, article 101546, 2020.

[19] R. Naveenkumar, M. Ravichandran, B. Stalin et al., "Comprehensive review on various parameters that influence the performance of parabolic trough collector," *Environmental Science and Pollution Research*, vol. 28, no. 18, article 13439, pp. 22310–22333, 2021.

[20] W. D. Wong-Ángel, L. Téllez-Jurado, J. F. Chávez-Alcalá, E. Chavira-Martínez, and V. F. Verduzco-Cedeño, "Effect of copper on the mechanical properties of alloys formed by powder metallurgy," *Materials & Design*, vol. 58, pp. 12–18, 2014.

[21] X. Li, G. Ma, P. Jin, L. Zhao, J. Wang, and S. Li, "Microstructure and mechanical properties of the ultra-fine grained ZK60 reinforced with low content of nano-diamond by powder metallurgy," *Journal of Alloys and Compound*, vol. 778, pp. 309–317, 2018.

[22] K. Yoganandam, V. Shanmugam, A. Vasudevan et al., "Investigation of dynamic, mechanical, and thermal properties of *Calotropis procera* particle-reinforced PLA biocomposites," *Advances in Materials Science and Engineering*, vol. 2021, Article ID 2491489, 7 pages, 2021.

[23] L. Liu, R. Bao, J. Yi, and D. Fang, "Fabrication of CNT/Cu composites with enhanced strength and ductility by SP combined with optimized SPS method," *Journal of Alloys and Compounds*, vol. 747, pp. 91–99, 2018.

[24] H. Wang, Z. H. Zhang, Z. Y. Hu et al., "Improvement of interfacial interaction and mechanical properties in copper matrix composites reinforced with copper coated carbon nanotubes," *Materials Science Engineering A*, vol. 715, pp. 163–173, 2018.

[25] P. Yang, X. You, J. Yi et al., "Simultaneous achievement of high strength, excellent ductility, and good electrical conductivity in carbon nanotube/copper composites," *Journal of Alloys and Compounds*, vol. 752, pp. 431–439, 2018.

[26] M. T. Alam, S. Arif, and A. H. Ansari, "Wear behaviour and morphology of stir cast aluminium/SiC nanocomposites," *Materials Research Express*, vol. 5, no. 4, article 045008, pp. 1–24, 2018.

[27] M. R. Akbarpour, S. Alipour, M. Farvizi, and H. S. Kim, "Mechanical, tribological and electrical properties of Cu-CNT composites fabricated by flake powder metallurgy method," *Archives of Civil and Mechanical Engineering*, vol. 19, no. 3, pp. 694–706, 2019.

[28] C.-W. Nan and R. Birringer, "Determining the Kapitza resistance and the thermal conductivity of polycrystals: a simple model," *Physical Review B*, vol. 57, no. 14, pp. 8264–8268, 1998.

[29] S. Sivasankaran, K. Sivaprasad, R. Narayanasamy, and V. K. Iyer, "Synthesis, structure and sinter- ability of 6061 AA100 –x–xwt.% TiO_2 composites prepared by high-energy ball milling," *Journal of Alloys and Compounds*, vol. 491, no. 1-2, pp. 712–721, 2010.

[30] A. K. Shukla, N. Nayan, S. V. S. N. Murty et al., "Processing of copper-carbon nanotube composites by vacuum hot pressing technique," *Materials Science and Engineering: A*, vol. 560, pp. 365–371, 2013.

[31] V. M. Kumar and C. V. Venkatesh, "Evaluation of microstructure, physical and mechanical properties of Al 7079–AlN metal matrix composites," *Materials Research Express*, vol. 6, no. 12, article 126503, 2019.

[32] M. P. Reddy, R. A. Shakoor, G. Parande et al., "Enhanced performance of nano-sized SiC reinforced Al metal matrix nanocomposites synthesized through microwave sintering and hot extrusion techniques," *Progress in Natural Science: Materials International*, vol. 27, no. 5, pp. 606–614, 2017.

[33] P. R. Matli, U. Fareeha, R. A. Shakoor, and A. M. A. Mohamed, "A comparative study of structural and mechanical properties of Al-Cu composites prepared by vacuum and microwave sintering techniques," *Journal of Materials Research and Technology*, vol. 7, no. 2, pp. 165–172, 2018.

[34] P. Zhang, J. Jie, Y. Gao et al., "Preparation and properties of TiB_2 particles reinforced Cu-Cr matrix composite," *Materials Science and Engineering: A*, vol. 642, pp. 398–405, 2015.

[35] J. H. Nie, C. C. Jia, X. Jia, Y. Li, Y. F. Zhang, and X. B. Liang, "Fabrication and thermal conductivity of copper matrix composites reinforced by tungsten-coated carbon nanotubes," *International Journal of Minerals, Metallurgy and Materials*, vol. 19, no. 5, pp. 446–452, 2012.

[36] S. Arivukkarasan, V. Dhanalakshmi, B. Stalin, and M. Ravichandran, "Mechanical and tribological behaviour of tungsten carbide (WC) reinforced aluminium LM4 matrix composites," *Particulate Science and Technology*, vol. 36, pp. 967–973, 2018.

[37] C. Zou, Z. Chen, H. Kang et al., "Study of enhanced dry sliding wear behavior and mechanical properties of Cu- TiB_2 composites fabricated by in situ casting process," *Wear*, vol. 392-393, pp. 118–125, 2017.